Solid State Communications 149 (2009) 1212–1215

Contents lists available at ScienceDirect

Solid State Communications

journal homepage: www.elsevier.com/locate/ssc

Parity violation in a single domain of spin-triplet Sr_2RuO_4 superconductors

H. Nobukane [a,*], K. Inagaki [a,b], K. Ichimura [a,b], K. Yamaya [a,b], S. Takayanagi [a,b], I. Kawasaki [c], K. Tenya [d], H. Amitsuka [b,c], K. Konno [a,b], Y. Asano [a,b], S. Tanda [a,b]

[a] Department of Applied Physics, Hokkaido University, Sapporo 060-8628, Japan

[b] The 21st Century COE Program "Topological Science and Technology" from the MEXT of Japan, Hokkaido University, Sapporo 060-8628, Japan

[c] Department of Physics, Hokkaido University, Sapporo 060-0810, Japan

[d] Department of Education, Shinshu University, Nagano 380-8544, Japan

ARTICLE INFO

Article history:
Received 26 December 2008
Received in revised form
8 April 2009
Accepted 24 April 2009 by S. Miyashita
Available online 3 May 2009

PACS:
73.23.-b
74.70.Pq
74.78.Na

Keywords:
A. Spin-triplet superconductor
D. Parity violation
E. Electric transport

ABSTRACT

We observed an unconventional parity-violating vortex in single domain Sr_2RuO_4 single crystals using a transport measurement. The current–voltage characteristics of submicron Sr_2RuO_4 show that the induced voltage has anomalous components which are *even* functions of the bias current. The results may suggest that the vortex itself has a helical internal structure characterized by a Hopf invariant (a topological invariant). We also discuss that the hydrodynamics of such a helical vortex causes the parity violation to retain the topological invariant.

A quantized vortex is a topological matter in superconductors and superfluids. In metallic superconductors, the Abrikosov vortex is characterized only by an integer winding number of phase. In unconventional superconductors, the superfluid of ^{3}He and spinor cold atoms, internal degrees of freedom of the order parameter enrich the variety of vortices [1–3]. Although a number of theoretical studies have predicted the existence of such unconventional vortices, experimental confirmation of them is still limited to several studies such as NMR spectroscopy of ^{3}He and imaging of spinor cold atoms [4,5]. Here a Cooper pair in spin-triplet superconductors has electric charge $2e$. Thus one can resolve the dynamics of unconventional vortices through electric transport. We will address this issue in the present Letter.

Sr_2RuO_4 [6] is a promising spin-triplet chiral p-wave superconductor candidate (i.e., spin $S = 1$ and orbital angular momentum $L = 1$). Since two states with different chirality degenerate in the ground state, bulk Sr_2RuO_4 is considered to have chiral domain structures. The transport properties have been studied in relation to Josephson interferometry using bulk Sr_2RuO_4 crystals to determine the symmetry of Cooper pairs and measure the dynamics of the chiral domains [7,8]. These experimental data on bulk Sr_2RuO_4 should be considered as a result of ensemble averaging over possible chiral domain configurations. Thus we need a small enough sample of Sr_2RuO_4 rather than the domain size to study phenomena that are peculiar to a single chiral domain such as dynamics of a single chiral domain, spin supercurrent, and unconventional vortices [9–11]. Transport measurements, however, have never been carried out yet in a single domain because it is also difficult to attach electrical contacts to submicron Sr_2RuO_4 crystals.

In this Letter, we will report an anomalous property of the current–voltage (I–V) characteristics in a single domain of Sr_2RuO_4. The creation of vortices gives a finite resistivity even when the temperature is well below the superconducting transition temperature. In four-terminal measurements, the induced voltage V is usually an *odd* function of the bias current I. Namely, V changes its sign when we flip the direction of current to the opposite direction, which implies parity conservation [12]. However, we find in submicron Sr_2RuO_4 samples that V has anomalous components which are *even* functions of I. The existence of the anomalous components means that positive voltage is detected regardless of the current direction and suggests the violation of parity [12]. To understand the nature of the anomalous I–V characteristics, we consider a simple

* Corresponding author. Tel.: +81 11 706 7293; fax: +81 11 706 6154.
E-mail address: nobukane@eng.hokudai.ac.jp (H. Nobukane).

0038-1098/$ – see front matter
doi:10.1016/j.ssc.2009.04.022

model of a vortex which has a helical internal structure characterized by a Hopf invariant. We also show that hydrodynamics of such a helical vortex violates the parity to retain the topological invariant.

To obtain submicron Sr_2RuO_4 single crystals, we synthesized Sr_2RuO_4 crystals with a solid phase reaction and then determined the crystal structure of Sr_2RuO_4 and the concentration of impurities. We prepared $SrCO_3$ and RuO_2 (both 99.9%, Kojundo Chem.) powders. The mixed powder was then heated at 990 °C for 60 h. The mixture was cooled gradually from 990 °C to 450 °C over 6 h. The samples were kept at 450 °C for 12 h to introduce oxide into the crystals and then cooled down slowly at room temperature. The structure of the Sr_2RuO_4 crystals was analyzed by using X-ray power diffraction (Rigaku Diffractometer RINT 2200HK) with Cu $K\alpha$ radiation. The observed peaks fitted a body-centered tetragonal unit cell of the K_2NiF_4 type with lattice constants $a = b = 3.867$ (± 0.004) Å and $c = 12.73$ (± 0.01) Å [13]. The result of secondary ion-microprobe mass spectrometry (SIMS) shows that the concentration of Al in the sample is less than 100 ppm, while the superconductivity of Sr_2RuO_4 is destroyed by nonmagnetic impurities [14].

We selected submicron Sr_2RuO_4 single crystals from the observations of chemical composition and crystallinity. The samples were dispersed in dichloroethane by sonication and deposited on an oxidized Si substrate. We found typical samples in diameter of about 50 nm–500 μm. Energy dispersion spectroscopy (EDS; EX-64175 JMU, JEOL) was used to determine the components of the submicron samples on the substrate. The molar fraction of the Sr and Ru elements was 2:1. We also confirmed that the dispersed crystals had neither boundaries nor ruthenium inclusions on the sample surface by observing the crystal orientation using the electron backscatter diffraction pattern (EBSP; OIM TSL [15]).

On the analyzed Sr_2RuO_4, we fabricated gold electrodes using overlay electron beam lithography. Inset (a) in Fig. 1 shows a micrograph of our samples. The sample size is 2.50 μm × 1.88 μm × 0.10 μm. The sample electrode spacing is 0.63 μm. Since the fabricated sample surface may have the insulator surface of the layer crystals and the residual resist between the sample and the gold electrodes, it is difficult to form an electrical contact. Therefore we performed a welding using electron beam irradiation [16]. We heated each electrode on the sample for 15 s with a beam current irradiation of 2×10^{-7} A. As the result, we succeeded in greatly reducing the contact resistance below 10 Ω at room temperature.

The measurements were carried out in a dilution refrigerator (Kelvinox, Oxford) with a base temperature of 60 mK. All measurement leads were shielded. The lead lines were equipped with low pass RC filters ($R = 1$ kΩ, $C = 22$ nF). In the DC measurements, a bias current was supplied by a precise current source (6220, Keithley) and the voltage was measured with a nanovoltmeter (182, Keithley) using four-terminal measurements.

We measured the temperature dependence of the resistivity in the submicron Sr_2RuO_4. Inset (b) of Fig. 1 shows the temperature dependence of the resistivity in the ab plane from room temperature down to 4.2 K. Fig. 1 shows that the resistivity $\rho_{ab}(4\,\mathrm{K}) = 6.0\,\mu\Omega$ cm. This value is larger than the bulk resistivity by about three times [14]. We estimated the resistivity ρ_{ab} from the sample size. Since Sr_2RuO_4 has anisotropic resistivity $\rho_{ab} \approx \rho_c \times 10^{-3}$ μΩ cm, the resistivity ρ_{ab} may actually be smaller than the estimation. Here the ratio $\rho_{ab}(300\,\mathrm{K})/\rho_{ab}(4\,\mathrm{K}) \sim 40$ is comparable to that of the bulk used in Ref. [6]. Hence we consider there is no degradation of the sample by the solvent. Fig. 1 also shows a transition temperature of $T_c = 1.69$ K and a broader transition temperature width of $\Delta T \approx 200$ mK. There was no decrease of the resistivity when a magnetic field of 3000 G was applied

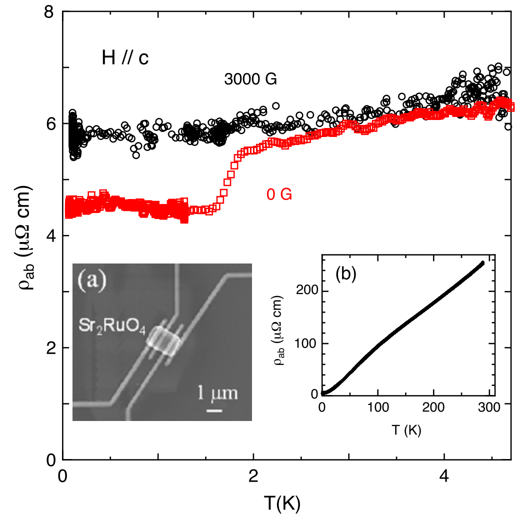

Fig. 1. Temperature dependence of resistivity of submicron Sr_2RuO_4 in zero magnetic field (0 G) and in a magnetic field ($H = 3000$ G) applied parallel to the c axis. Flat tail resistivity can be seen at low temperatures below $T_c = 1.69$ K. Inset (a) shows a micrograph of a submicron Sr_2RuO_4 single crystal connected to gold electrodes. Inset (b) displays the temperature dependence of the resistivity in the ab plane from room temperature down to 4.2 K.

parallel to the c axis. Our sample shows neither suppression of T_c nor enhancement to 3 K [14,17]. Here the resistivity retained its flat tail below T_c. The result shows that the flow of vortices can occur by quantum fluctuations of the superconducting phase θ [18]. The results show transport properties of the submicron Sr_2RuO_4 single crystals because a broader transition temperature width and quantum fluctuations of the phase are characteristic of mesoscopic superconductors [19].

We observed anomalous I–V characteristics in zero magnetic field. Fig. 2(a) shows I–V curves at several temperatures with typical flat tail resistances of $R^* \approx 0.16$ Ω. In general, the voltage in I–V curves for metals, quantum Hall systems and Josephson junction is always an *odd* function of the bias current, which is a result of parity conservation. Surprisingly, V is not an *odd* function of I at all. In what follows, we define anomalous nonlinear voltage (ANV) as the component of measured voltage given by an *even* function of I. An ANV implies the violation of parity. The amplitude of the ANV increases with decreasing temperature in zero magnetic field and shows a maximum below 200 mK. In order to eliminate completely the possibility of instrument malfunction in the DC measurements, I–V curves were measured with a microvoltmeter (AM 1001, Ohkura Electric Co.) with a battery-powered current source. Furthermore, in the AC measurements, we also measured the differential resistance dV/dI as a function of the bias current using lock-in techniques. Fig. 2(b) clearly shows that dV/dI has an *odd* component of I. The parity violation in the I–V characteristics is confirmed in both the DC and AC measurements. Moreover, we confirmed that the anomalous effect was reproduced in several samples.

To analyze the ANV in more detail, we subtract the linear part (ohmic contribution to voltage) from the I–V curves in Fig. 2(a). The results are shown in Fig. 3. We clearly find that the ANV is symmetric with respect to the zero bias current, (i.e., $V_1(+I) = V_1(-I)$). Here the voltage V_1 represents the ANV of the induced voltage $V = R^*I + V_1$. These curves are described well by a Lorentzian curve, as shown by the lines.

We discuss the physical difference between parity-violating I–V characteristics and negative resistance. Negative resistance itself is an unusual phenomenon. The phenomenon, however, is possible. It is instructive to compare our result to the negative resistance of mesoscopic charge density waves (CDWs) reported

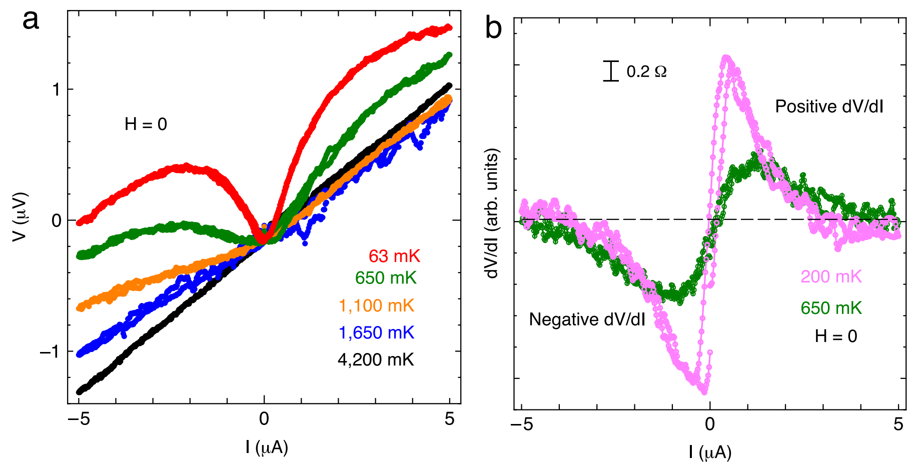

Fig. 2. (a): Results of DC measurements. Voltage V is plotted as a function of bias current I in the absence of magnetic field for several choices of temperatures. The amplitude of the ANV increases with decreasing temperature and shows a maximum below 200 mK. (b): Results of AC measurements. The differential resistance dV/dI versus bias current I is shown at $T = 200$ mK and 650 mK. The upper and lower regions of the transverse dotted line represent positive and negative differential resistance, respectively. As shown in (a) and (b), parity violation is confirmed in two different measurements.

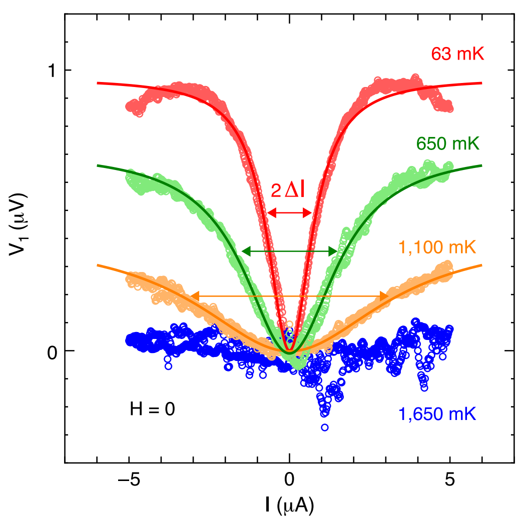

Fig. 3. The anomalous nonlinear voltage (ANV) which is described by the voltage V_1 is extracted from I–V characteristics in Fig. 2, where the lines are Lorentzian fitting curves. The half-widths ΔI of the fitting curves are represented by two-headed arrows. We eliminated the offset voltage of 0.13 μV in order to discuss the ANV.

in Ref. [20]. In their report, the negative resistance was attributed to the backflow of quasiparticles of the CDW. This does not relate to parity violation of the I–V curves. On the other hand, our observation of $V_1(+I) = V_1(-I)$ in the submicron Sr_2RuO_4 is a parity violation, which is a qualitatively different phenomenon from the CDW case. The parity violation of I–V curves must naturally include both negative resistance and negative differential resistance. In addition, since the measurement was carried out in the four-terminal configuration, the observation does not violate any basic laws, such as energy conservation. From the reasons, we focus on discovery of the parity violation.

What is the origin of the ANV in the I–V characteristics? The flat tail of resistivity (which often appears in superconductors owing to quantum fluctuations of the phase [18]) shown in Fig. 1 may suggest that the flow of vortices causes the ANV. However, the dynamics of the usual Abrikosov vortex in type-II superconductors cannot explain the parity violation in the I–V curves. Therefore we need to consider unconventional vortices characterized by $\vec{l}$ and $\vec{d}$ textures as in superfluid ^{3}He-A. Here the $\vec{l}$ vector represents the direction of the pair angular momentum parallel to the c axis and the $\vec{d}$ vector describes the spin configuration of a pair. These internal degrees of freedom are characters of spin-triplet p-wave superconductivity. Kerr effect measurements of Sr_2RuO_4 [21] and Josephson tunneling measurements [8] respectively suggested the chiral domain size to be 50 ∼ 100 μm and 1 μm. Recently, an experiment on the 3 K phase of Sr_2RuO_4 also revealed that the domain size is ∼10 μm [22]. Since our sample electrode spacing is 0.63 μm, our sample is considered to have a single chiral domain. The spin degree of freedom represented by $\vec{d}$ allows the formation of $\vec{d}$ textures in the single domain. In bulk Sr_2RuO_4, the spin–orbit interaction favors the alignment of $\vec{d}$ and $\vec{l}$ in zero magnetic field. Knight shift measurements have recently suggested that a magnetic field $H > 200$ G may neutralize the interaction [23]. However, in submicron Sr_2RuO_4, quantum fluctuations of the phase disturb the alignment of $\vec{d}$ in a particular direction. Thus $\vec{d}$-textures would be possible in a single domain of Sr_2RuO_4.

In what follows, we consider a spin-triplet Cooper pair as a spin-1 boson with charge $2e$. Babaev theoretically predicted that the ground state of such a boson system can have magnetic spin textures $\vec{\boldsymbol{s}}$ characterized by a topological invariant known as helicity in zero magnetic field [10]. The equivalence between gauge transformation and spin rotation causes a term

$$B_k{}^2 = \left(-\frac{cM}{4e^2 n}[\nabla_i J_j - \nabla_j J_i] + \frac{\hbar c}{4e}(\vec{\boldsymbol{s}} \cdot \nabla_i \vec{\boldsymbol{s}} \times \nabla_j \vec{\boldsymbol{s}})\right)^2 \qquad (1)$$

in the Ginzburg–Landau energy functional, where $\nabla_i = \frac{d}{dx_i}$, $\boldsymbol{J}$ is the electric current, M is the mass of a boson, and n is the boson density. In Ref. [24], the authors described a nontrivial topological structure in the simplest toroidal knot soliton. The main distinction between knotted solitons in spin-triplet superconductors and the topological defects of ^{3}He in Ref. [25] is the appearance of terms $\propto (\vec{\boldsymbol{s}} \cdot \nabla_i \vec{\boldsymbol{s}} \times \nabla_j \vec{\boldsymbol{s}})^2$. This results in the knotted solitons being protected against shrinkage by an energy barrier. According to Ref. [10], the size of the knotted soliton is comparable to the magnetic penetration length. Our sample satisfies this requirement about the size. We note that the sample size ≈1 μm and $\lambda_{ab} \approx 152$ nm.

In the Sr_2RuO_4 single domain, a helical vortex could be created by the spin degree of freedom. If we accept the existence of such helical vortices, the anomalous I–V characteristics could be understood as a result of the conservation of a topological invariant in the helical vortex. Now let us consider the *hydrodynamics* of a helical vortex. In the initial state of the bias current $I = 0$, the helical vortex does not move. When we switch on a bias current $I > 0$, a clockwise helical vortex ($\omega > 0$) exerts the Magnus force in a

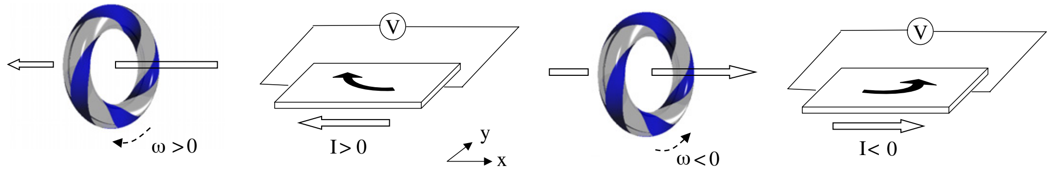

(a) Clockwise. (b) Counterclockwise.

Fig. 4. A model of a vortex which violates parity. A topological invariant features a helical structure of the vortex. The blue spiral line on the torus represents a magnetic helical structure of spin texture described by $(\vec{s} \cdot \nabla_i \vec{s} \times \nabla_j \vec{s})$. Under the bias current, the spin texture around the torus moves periodically from the inside to the outside. Open arrows represent the current flow I. Solid arrows show the direction of the Magnus force. (For interpretation of the references to colour in this figure legend, the reader is referred to the web version of this article.)

direction perpendicular to the current, as shown in Fig. 4(a). Here $+y$ indicates the direction of the Magnus force. On the other hand, for a bias current $I < 0$, the helical vortex changes its rotation frequency from clockwise ($\omega > 0$) to counterclockwise ($\omega < 0$) in order to retain the topological invariant. As a consequence, the counterclockwise helical vortex also exerts a Magnus force in the $+y$ direction as shown in Fig. 4(b). Thus the direction of the Magnus force is independent of the direction of the bias current. According to Josephson's equation, the motion of a vortex in the $+y$ direction induces a voltage across the sample of Sr_2RuO_4 in the x direction. In this way, the presence of helical vortices explains the ANV.

Let us discuss the amplitude voltage of the ANV using the simple energy conversion formula $eV \sim \mu_B B$, where μ_B is the Bohr magneton, in the I–V curves. The energy of the amplitude voltage $V_1 = 0.97\ \mu V$ of the ANV at 63 mK is comparable to the energy of the magnetic field $H \approx 200$ G which neutralizes the spin–orbit interaction in bulk Sr_2RuO_4 [23]. Thus we consider that the amplitude voltage of the ANV may exhibit the contribution of the helical vortices.

Finally we briefly discuss the meaning of this experiment. Although Sr_2RuO_4 is a spin-triplet superconductor candidate, this conclusion is still under debate. We show in this Letter that a Cooper pair in Sr_2RuO_4 has a spin degree of freedom. Thus our results exhibit a possibility of spin-triplet symmetry [26]. When helical vortices exist in a sample, such topological defects may affect the Hall conductivity. This inference stems from an analogy between the Chern–Simons term in the quantum Hall effect and the helical spin term in Babaev's argument. Thus we believe that transport experiments which are sensitive to probe geometry would display more interesting phenomena reflecting the internal degree of freedom of a Cooper pair.

In summary, we have observed an unconventional vortex which violates the parity in a single domain of Sr_2RuO_4 using a transport measurement. The I–V characteristics of submicron Sr_2RuO_4 show that the voltage has anomalous components which are *even* functions of the bias current. We consider a vortex with a helical internal structure characterized by a Hopf invariant. The invariant of the vortex is protected while the vortex is moving under the bias current. By a simple argument, we show that the hydrodynamics of the helical vortex causes the anomalous I–V characteristics to retain the topological invariant.

Acknowledgements

The authors thank A. Ishii, S. Tsuchiya, T. Toshima, T. Matsuura, T. Kuroishi, and D. Meacock for experimental help and useful discussions. We also are grateful to Y. Maeno, and T. Matsuyama. H.N. acknowledges support from the Japan Society for the Promotion of Science.

References

[1] M. Sigrist, K. Ueda, Rev. Mod. Phys. 63 (1991) 239.
[2] G.E. Volovik, Exotic Properties of Superfluid ^{3}He, World Scientific, Singapore, 1992.
[3] T.-L. Ho, Phy. Rev. Lett. 81 (1998) 742;
T. Ohmi, K. Machida, J. Phys. Soc. Jpn. 67 (1998) 1822.
[4] V.M.H. Ruutu, Ü. Parts, M. Krusius, J. Low Temp. Phys. 103 (1996) 331.
[5] J. Stenger, S. Inouye, D.M. Stamper-Kurn, H.-J. Miesner, A.P. Chikkatur, W. Ketterle, Nature 396 (1998) 345.
[6] A.P. Mackenzie, Y. Maeno, Rev. Mod. Phys. 75 (2003) 657.
[7] K.D. Nelson, Z.Q. Mao, Y. Maeno, Y. Liu, Science 306 (2004) 1151.
[8] F. Kidwingira, J.D. Strand, D.J.V. Harlingen, Y. Maeno, Science 314 (2006) 1267.
[9] Y. Asano, Phys. Rev. B 72 (2005) 092508; Phys. Rev. B 74 (2006) 220501(R).
[10] E. Babaev, Phys. Rev. Lett. 88 (2002) 177002.
[11] S.B. Chung, H. Bluhm, E.-A. Kim, Phys. Rev. Lett. 99 (2007) 197002.
[12] Here we apply a simple argument as follows. Both the electric field E (voltage drop V per unit length) and electric current I have odd parity, (i.e., change their signs under the space inversion). Thus a relation $V = \sum_{n=1}^{\infty} a_n I^{2n+1}$ is usually expected. However, when a relation $V = \sum_n a_n I^{2n+1} + \sum_m b_m 2I^{2m}$ holds with $b_m \neq 0$, V and I cannot have odd parity at the same time. In this Letter, we claim that some defect (vortex) of parity nonconservation causes such anomalous I–V characteristics.
[13] F. Lichtenberg, A. Catana, J. Mannhart, D.G. Schlom, Appl. Phys. Lett. 60 (1991) 1138.
[14] A.P. Mackenzie, R.K. Haselwimmer, A.W. Tyler, G.G. Lonzarich, Y. Mori, S. Nishizaki, Y. Maeno, Phys. Rev. Lett. 80 (1998) 161.
[15] B.L. Adams, S.I. Wright, K. Kunze, Metall. Trans. 24A (1993) 819.
[16] K. Inagaki, T. Toshima, S. Tanda, K. Yamaya, Appl. Phys. Lett. 86 (2005) 073101.
[17] Y. Maeno, T. Ando, Y. Mori, E. Ohmichi, S. Ikeda, N. NishiZaki, S. Nakatsuji, Phys. Rev. Lett. 81 (1998) 3765.
[18] E. Chow, P. Delsing, D.B. Haviland, Phy. Rev. Lett. 81 (1998) 204;
H.M. Jaeger, D.B. Haviland, B.G. Orr, A.M. Goldman, Phys. Rev. B 40 (1989) 182.
[19] P.G. de Gennes, Superconducting of Metals and Alloys, Benjamin, New York, 1969.
[20] H.S.J. van der Zant, E. Slot, S.V. Zaitsev-Zotov, S.N. Artemenko, Phys. Rev. Lett. 87 (2001) 126401.
[21] J. Xia, Y. Maeno, P.T. Beyersdorf, M.M. Fejer, A. Kapitulnik, Phys. Rev. Lett. 97 (2006) 167002.
[22] H. Kambara, S. Kashiwaya, H. Yaguchi, Y. Asano, Y. Tanaka, Y. Maeno, Phys. Rev. Lett. 101 (2008) 267003.
[23] H. Murakawa, K. Ishida, K. Kitagawa, Z.Q. Mao, Y. Maeno, Phys. Rev. Lett. 93 (2004) 167004.
[24] E. Babaev, L.D. Faddeev, A.J. Niemi, Phys. Rev. B 65 (2002) 100512(R).
[25] G.E. Volovik, V.P. Mineev, Sov. Phys. JETP 46 (1977) 401.
[26] At present, we cannot distinguish between two possibilities of spin ($S = 1$) and orbital angular momentum ($L = 1$). As other possibilities, we also should consider the physical aspect of a chiral p-wave pairing for our experimental data. In what follows, we give three Letters which are related to a chiral pairing. K. Miyake, O. Narikiyo, Phys. Rev. Lett. 83 (1999) 1423;
R. Arita, S. Onari, K. Kuroki, H. Aoki, Phys. Rev. Lett. 92 (2004) 247006;
M. Takigawa, M. Ichioka, K. Kuroki, Y. Tanaka, Phys. Rev. B 72 (2005) 224501.